MATHEMATICAL MODELLING OF SIGNALLING IN *DICTYOSTELIUM DISCOIDEUM*

JONATHAN A. SHERRATT[1], JOHN C. DALLON[1], THOMAS HÖFER[2] AND PHILIP K. MAINI[3]

[1]*Department of Mathematics, Heriot-Watt University, Edinburgh EH14 4AS, UK*

[2]*Institute of Biophysics, Humboldt University of Berlin, Invalidenstrasse 42, D-10115 Berlin, Germany*

[3]*Centre for Mathematical Biology, Mathematical Institute, 24–29 St Giles', Oxford OX1 3LB, UK*

INTRODUCTION

The cellular slime mould *Dictyostelium discoideum* (*D. discoideum*) has a remarkable life cycle, incorporating many key features of morphogenesis in higher organisms, including chemotaxis, cell differentiation and multicellular organization. In starvation conditions, the unicellular amoebae aggregate into a multicellular slug (containing about 10^5 cells), which is capable of coordinated movement towards chemical and light sources. Within the slug, cells begin to differentiate and sort into 'prestalk' (about 20%) and 'prespore' (about 80%); at some point the slug becomes stationary, and these cells form the stalk and spores of a 'fruiting body', from which individual spore cells are dispersed when conditions become more favourable. For detailed reviews of this life cycle, see Bonner (1982) and Devreotes (1982). The experimental accessibility of *D. discoideum*, along with the key features mentioned above, has led to its widespread adoption as a prototype morphogenetic system. What was once thought of as a simple system has become a rich source of information for the processes of gene regulation during development, signal transduction pathways, amoeboidal movement and chemotaxis. The aggregation stage has been particularly well studied. The key to this process is intercellular signalling by cyclic adenosine 3′,5′-monophosphate (cAMP). Starvation causes a small number of cells, distributed throughout a population, to act as pacemakers, emitting cAMP periodically (Raman *et al.*, 1976). Surrounding cells move towards these pacemakers because of a chemotactic response to cAMP; they also secrete cAMP themselves in an autocatalytic manner, propagating the signal across the spatial domain. The waves of cAMP take the form either of target patterns, concentric circles, or spirals.

Initial mathematical models for *D. discoideum* morphogenesis focused on the kinetics of cAMP, both intra- and extracellular, and the cAMP-receptor on the cell surface (Goldbeter & Segel, 1977). Crucially, investigation of the

spatiotemporal dynamics of this reaction predicted spiral wave formation (Hagan & Cohen, 1981; Tyson *et al.*, 1989), in agreement with the spiral patterns seen in a field of aggregating *D. discoideum* amoebae. A number of other aspects of *D. discoideum* biology have also been extensively modelled mathematically, including slug migration (Odell & Bonner, 1986), cell sorting within the slug (Meinhardt, 1983), mound formation at the end of aggregation (Vasiev *et al.*, 1989; Levine *et al.*, 1997), and the formation of cellular streams during aggregation. This chapter will concentrate on this last issue, and review some of the mathematical models proposed during the past few years. The reasons for this focus are as follows. First, it is an excellent example of the ability of biochemical signalling in amoebae to generate coordinated behaviour, and secondly, it is one of a very few areas of cell biology to which a wide variety of different mathematical modelling approaches have been applied, and comparison of the results of these approaches provides valuable insight into the biological process.

The term 'streaming' refers to the fact that, as *D. discoideum* cells move into the aggregation centre, they do so not as a uniform field, but rather in discrete streams, separated by about 50 μm (Fig. 1). The wide variety of mathematical models for this phenomenon are all based on the inclusion of cell movement into existing models for the spatiotemporal dynamics of cAMP. This section briefly reviews these dynamics and their mathematical modelling.

The basic reason for cAMP wave propagation during *D. discoideum* aggregation is that cAMP dynamics fall into a category known as an 'excitable system'. This refers to the fact that behaviour occurs on two different time scales; the processes involved in the production and release of cAMP occurring more rapidly than the competing process which turns off cAMP production. The competing process eventually wins and 'resets' the system to the original state of very low cAMP production. However, the difference in time scales generates 'cycles' of cAMP concentration. To explain this, it is assumed that an initial moderate level of cAMP is added uniformly to a field of *D. discoideum* amoebae. This stimulates the amoebae to produce and release cAMP, causing cAMP levels to increase even further, until the much slower inhibition of the production 'catches up'. This returns the amoebae to a low cAMP producing state, so that the cAMP concentration returns to its original level. In reality, however, cAMP is added not uniformly, but at one point in space, by a pacemaker cell. The above cAMP-cycle then occurs in the immediate vicinity of the pacemaker. However, during the phase of this cycle at which cAMP levels are high, sufficient cAMP diffuses into the surrounding regions to stimulate other amoebae, initiating a cAMP cycle there, and this process is repeated throughout the field of cells. It is this series of phase-lagged cAMP cycles that constitutes the observed periodic and spiral waves of cAMP.

A simple mathematical representation of cAMP dynamics, which highlights its excitability, was developed by Martiel and Goldbeter (1984). The

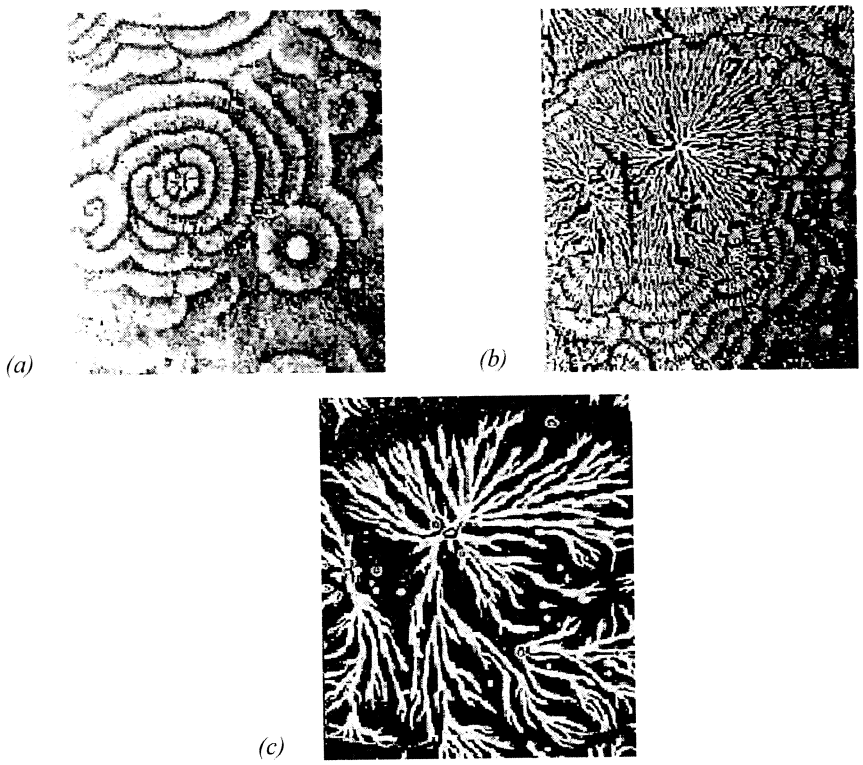

Fig. 1. Aggregation of *Dictyostelium* (str NP377) on an agar plate, showing the formation of spiral cAMP waves which induce (*a*) cell movement, (*b*) the onset of cell streaming, and (*c*) the developed cell stream morphology in the whole aggregation territory. Pictures are taken *ca.* 15 min apart. The position of the cAMP waves in (*a*), (*b*) can be inferred from the different light scattering responses of elongated (moving) and rounded (stationary) cells; amoebae elongate under the influence of the cAMP waves and form the bright bands in the photograph. (Courtesy of P.C. Newell.)

model consists of differential equations for three variables, extracellular cAMP concentration (u), active cAMP-receptor concentration (v), and intracellular cAMP concentration (w):

$$\partial u/\partial t = k_1 w - k_2 u + D\nabla^2 u \tag{1a}$$

$$\partial v/\partial t = -f_1(u) + f_2(u) \cdot (1 - v) \tag{1b}$$

$$\partial w/\partial t = k_3 f_3(u, v) - k_4 w \tag{1c}$$

where

$$f_1(u) = \frac{k_5 + k_6 u}{1 + u} \quad f_2(u) = \frac{k_7 + k_8 u}{1 + k_9 u} \quad f_3(u, v) = \frac{k_{10}(1 + u)^2 + u^2 v^2}{k_{11}(1 + u)^2 + u^2 v^2}$$

Here f_1 and f_2 are kinetic rate functions for receptor desensitization and

resensitization respectively, and f_3 describes the activation of adenylate cyclase by bound and active receptors; the ks are positive constants. Numerical simulations of these equations, illustrating spiral waves, were presented by Tyson *et al.* (1989). A more mathematical account of spiral wave formation in an excitable system such as this is given in the book of Grindrod (1991).

The representation of signal transduction in the Martiel–Goldbeter model is extremely simplistic. A great deal is known about the details of cAMP dynamics. Briefly, the binding of cAMP to cell surface receptors induces excitation and adaptation of guanylyl cyclase and adenylyl cyclase, on time scales of seconds and minutes respectively. The first of these controls the chemotactic response of the amoeba (see below), while the second causes synthesis and secretion of cAMP. These processes are regulated by the G proteins in a complicated manner which is not yet fully understood. A mathematical model reflecting this level of detail was proposed by Tang and Othmer (1994, 1995) for the pathway involving adenylyl cyclase; their later paper simplifies the system to five differential equations, of the form

$$\frac{dw_1}{d\tau} = \alpha_4 u_2 - w_1 - \alpha_4 u_2 w_1 \tag{2a}$$

$$\frac{dw_2}{d\tau} = \beta_2\beta_3 c_2 u_4 - \beta_5 w_2 + \beta_6 c_3 w_3 - c_3\beta_4 u_1 w_2 - \beta_2\beta_3 c_2 u_4 (w_2 + c_3 w_3) \tag{2b}$$

$$\frac{dw_3}{d\tau} = -(\beta_5 + \beta_6) w_3 + \beta_4 u_1 w_2 \tag{2c}$$

$$\frac{dC_i}{d\tau} = \gamma_1\gamma_2 w_1 + \gamma_5(1 - w_1) - \gamma_4 \frac{C_i}{C_i + \gamma_3} - sr(C_i) \tag{2d}$$

$$\frac{\partial C_o}{\partial \tau} = \Delta_1 \nabla^2 C_o - \hat{\gamma}_9 \frac{C_o}{C_o + \gamma_8} + \frac{\rho}{1 - \rho}\left(sr(C_i) - \gamma_7 \frac{C_o}{C_o + \gamma_6}\right) \tag{2e}$$

where

$$u_1 = \frac{\alpha_0 C_o + (\beta_5 - \alpha_0 C_o) w_3}{\alpha_1 + \alpha_0 C_o + \beta_4 w_2} \quad u_2 = \frac{\alpha_2\alpha_3 c_1 u_1 (1 - w_1)}{1 + \alpha_4 + \alpha_2\alpha_3 c_1 u_1 - \alpha_4 w_1} \quad u_4 = \frac{\beta_0 C_o}{\beta_1 + \beta_0 C_o}$$

In these equations C_i represents internal cAMP, C_o external cAMP, u_1 (u_4) the fraction of stimulatory (inhibitory) receptors bound with cAMP, u_2 the fraction of the activated subunit of the stimulatory G protein, w_1 the activated adenylyl cyclase complex, w_2 a subunit of the hypothesized inhibitory G protein and w_3 represents a complex of w_2 and u_1. Further details of the signal transduction mechanism are reviewed by H. G. Othmer and P. Schaap (unpublished data).

A DISCRETE MODEL FOR *D. DISCOIDEUM* AGGREGATION

The phenomenon of cell streaming results from the interaction of the spatiotemporal dynamics of cAMP with the movement of *D. discoideum*

cells up gradients of cAMP. Mathematical models for streaming differ in two basic ways. First, they use representations of cAMP kinetics with various levels of detail, ranging from caricatures to fairly accurate accounts of the current level of knowledge. Secondly, models differ in the way in which the cell populations are represented, varying between continuum models which average over the cells, and discrete models in which individual cells are represented as discrete objects. Mathematically this latter difference is the most fundamental, giving completely different types of equation system. Two detailed models at opposite ends of both of these spectra will be discussed. In this section the model of Dallon and Othmer (1997) is described, in which a realistic representation of cAMP kinetics is used (taken from Tang & Othmer, 1994), and in which the *D. discoideum* amoebae are represented as discrete objects. In the following section the model of Höfer *et al.* (1995*a*,*b*) is described, which uses a caricature of cAMP dynamics and represents the amoebae as a continuous population. Various other models are mentioned in the Discussion.

When representing each amoeba individually, the key mathematical assumptions are those made on cell movement. In the work of Dallon and Othmer (1997), the following movement rules were used:

(i) The cell moves if the time derivative of the extracellular cAMP concentration is greater than $0.02\,\mu M\,min^{-1}$. This ensures that a triangular wave of cAMP of duration 200 s above baseline and amplitude 0.1 μM initiates movement.

(ii) All cells move for a fixed duration (100 s for wild-type cells) in the direction of the cAMP gradient at the cell when the motion started. This level of persistence is based on experimental observations of the time for which cells move during aggregation (Alcantara & Monk, 1974; Tomchick & Devreotes, 1981). However, it is somewhat arbitrary, and is an important parameter to vary in model simulations.

(iii) The cells move at a fixed speed of $30\,\mu m\,min^{-1}$, which is the maximum cell speed measured in experiments of Alcantara and Monk (1974). In reality, cells will move more slowly initially, speeding up as a result of successive stimulation by cAMP or when they form streams (Varnum *et al.*, 1985). However, such variations in speed would represent a significant increase in mathematical complexity.

Using these rules, Dallon and Othmer (1997) followed the movement of a fixed number of cells, varying between 120 000 and 160 000, in a $1\,cm^2$ area. In parallel with this cell tracking, the Tang–Othmer equations (2) were used to determine the concentration of cAMP and related variables. This combined system was solved numerically using techniques similar to the particle-in-cell method developed for combustion problems (details in Dallon & Othmer, 1997). Figure 2(*a*) shows a model simulation for parameter values corresponding to wild-type *D. discoideum*. The model

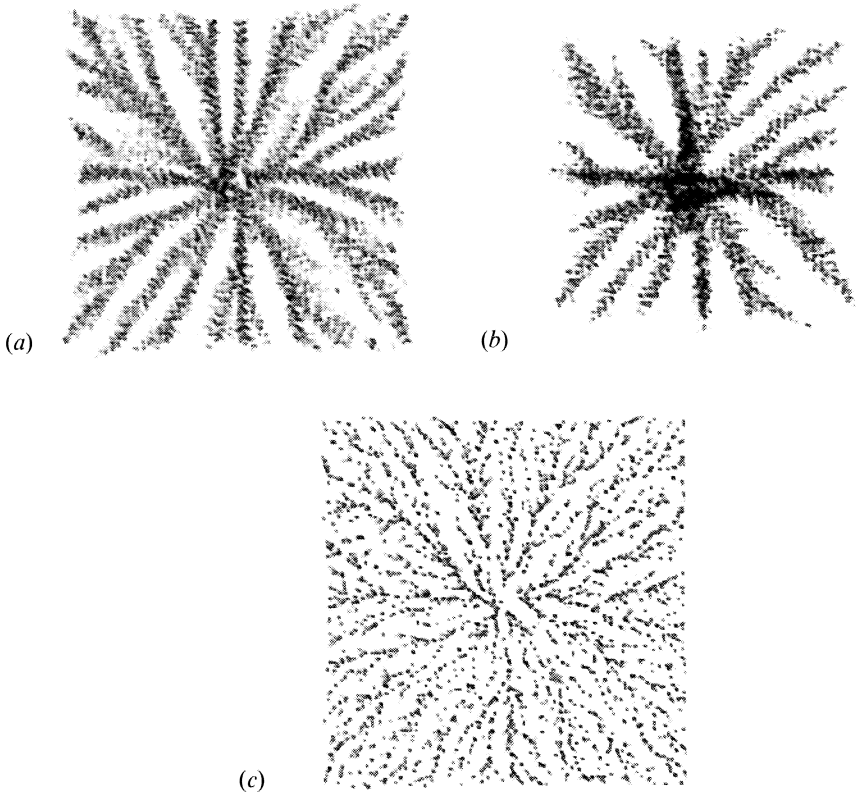

Fig. 2. Aggregation patterns for simulated wild-type (*a*) and mutant (*b*), (*c*) cells. (*a*) The predicted pattern for wild-type cells, with a movement duration of 100 s. (*b*) The pattern for *streamer F* mutants, with a movement duration of 500 s. (*c*) The pattern for *jittery* mutants, with movement duration 20 s. The solutions are shown after a model run of 95 min duration; cells in the centre are oscillatory, with parameter γ_2 ranging between 0.4 and 0.17.

predicts spiral waves of cAMP (not shown), with cell aggregation induced by the cAMP wave, and the formation of cell streams. Both this overall behaviour and the predicted space and time scales agree very closely with experimental observations.

The discrete nature of the model enables it to be used to predict the implications of mutations. Figure 2(*b*) shows a simulation corresponding to the *streamer F* mutant studied by Ross and Newell (1981); here, the time over which cells move between direction changes has been increased from 100 s (wild-type) to 500 s (*streamer F*). This change causes the cell streams to be fewer in number, but larger and more compact, again in close agreement with experimental observations. Figure 2(*c*) shows the results of reducing the duration of movement to 20 s; this is an artificial mutation, which Dallon and Othmer named *jittery*. In this case, thin and highly fragmented streams form

so that aggregation to the pacemaker does not occurs. These differences can be explained by reference to the time scale of a cAMP wave pulse, which takes about two minutes for both the wave front and wave back to move past a fixed point in space. Therefore, *jittery* cells reorient several times during the passage of a single cAMP pulse. Since these global waves of cAMP are the sum of small cAMP bursts from each cell, as described above, they can have very rough profiles, with several local maxima and minima. Reorienting several times during a wave front will cause the cell to become caught at a local maximum. In contrast, in the wild type cells, and to an even greater extent for the *streamer F* mutant, cell direction is primarily set in the wave-front and not reset until the cAMP pulse has passed.

A CONTINUOUS MATHEMATICAL MODEL

The representation of the *D. discoideum* amoebae as discrete objects in the model of Dallon and Othmer (1997) discussed above is relatively unusual within mathematical models for cell biology. Other examples are few: for example, work of Weliky *et al.* (1991) on *Xenopus* gastrulation, and the study of juxtacrine signalling by Collier *et al.* (1996); there are also some other examples of application to *D. discoideum* signalling that will be discussed later. These various discrete models have all been proposed by individual investigators, on a somewhat *ad hoc* basis. In contrast, an established body of theory exists for models of a 'continuum' type. In these, cells are not represented as discrete objects, but rather via a 'cell density', which denotes the number of cells per unit area at a point in the domain. Models of this type have a long history of application to developmental biology and medicine; see Murray (1989) for review. Höfer *et al.* (1995*a*) studied streaming using such a continuum representation of *D. discoideum* amoebae, coupled to the simple Martiel–Goldbeter representation of cAMP kinetics. In this section the model of Höfer *et al.* (1995*a*) is described and the results compared with those of Dallon and Othmer (1997).

Within a continuum model, cellular dynamics are represented by a 'conservation equation', in which the various contributions to overall cell movement are represented by separate terms. In the case of *D. discoideum* amoebae, there is a background level of random migration, in addition to directed movement up gradients of cAMP. Mathematically, this gives the equation:

$$\partial n/\partial t = \underbrace{\nabla \cdot [\mu(n)\nabla n]}_{\text{random migration}} - \underbrace{\nabla \cdot [\chi(v)n\nabla u]}_{\text{chemotaxis}} \tag{3}$$

where $n(\underline{x}, t)$ denotes the cell density; recall that $u(\underline{x}, t)$ and $v(\underline{x}, t)$ represent the concentrations of extracellular cAMP and active cAMP- receptor, respectively. It would be straightforward to include terms representing cell

division and death in this equation, but these are omitted because the extent of these processes is essentially negligible during aggregation. Höfer *et al.* (1994) studied equation 3 coupled to the Martiel–Goldbeter equations 1 for cAMP kinetics. The most immediate outcome of these simulations was an explanation for the so-called 'chemotactic wave paradox' (Soll *et al.*, 1993). As a pulse of cAMP passes an amoeba, it is observed to move in the wave front, but not in the wave back, giving significant cell movement in the opposite direction to that of the pulse. This is intuitively suprising, since there are equal (but opposite) cAMP gradients in both the wavefront and waveback; because the gradient in the waveback would promote movement with the cAMP pulse, the cell should spend longer in the waveback than in the wavefront, causing a small net movement in the same direction as the pulse. This contradiction was resolved by Höfer *et al.* (1994), using simulations of a slightly simplified version of equations (1, 3). Briefly, because the time scales of cell movement and desensitization to cAMP are similar for *D. discoideum*, the cell becomes sensitized while they are moving in the wavefront of the cAMP pulse, and by the time the waveback reaches the cell, it is no longer sensitive to cAMP gradients, so that little further movement occurs (illustrated in Fig. 3).

Having confirmed that the model predicts the correct timecourse of cell movement in cAMP gradients, Höfer *et al.* (1995*a*) used the model (1,3) to simulate aggregation on an agar plate; a typical example is illustrated in Fig. 4. Initially, a rotating spiral wave pattern of cAMP develops from a disrupted wave front, inducing cell movement towards the wave core. The interaction of the cAMP waves and cell chemotaxis then causes initial inhomogeneities in cell density to grow, leading to the formation of cell streams. This in turn disrupts the cAMP wave, which reinforces the streaming pattern. Thus this model predicts that the observed streaming pattern is the result of an instability along the length of an advancing front of cells, with cells gradually sorting into clumps, via movement up small cAMP gradients, as successive arms of the cAMP spiral wave move past them.

There are two very notable points of difference between the Höfer *et al.* (1995*a*) model, and that of Dallon & Othmer presented in the previous section. The first is that Höfer *et al.* (1995*a*) are unable to predict initiation of the spiral wave of cAMP. Rather, the spiral is induced rather artificially in simulations such as that illustrated in Fig. 4. This is common practice: studies such as those of Tyson *et al.* (1989) showed that cAMP dynamics are able to support spiral waves, but do not explain their initiation. In contrast, Dallon and Othmer's (1997) model does predict spiral wave generation, caused by small asymmetries in cell locations around pacemaker cells (see above). Subsequently, spiral wave generation has been demonstrated in continuum models, based on desynchronization of cells on the developmental path (Lauzeral *et al.*, 1997).

The second key difference between the models concerns mathematical tractability. The differential equations in terms of which the model of Höfer

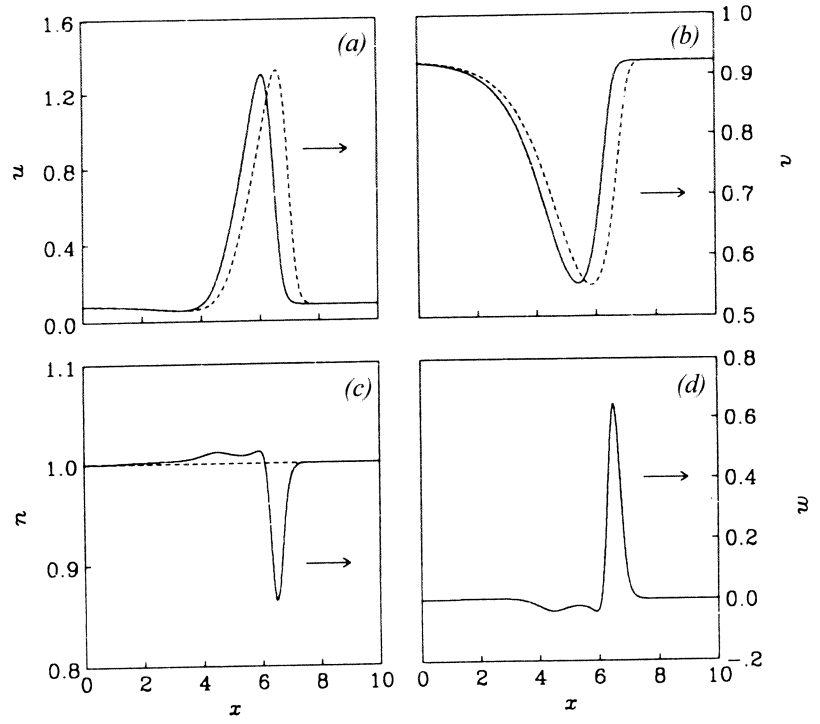

Fig. 3. Travelling pulse solutions of equations (1,3) in one space dimension (solid line), compared to wave solution of (1) with cell density n fixed at the value 1 (dashed line). (*a*) cAMP concentration, (*b*) fraction of active receptors, (*c*) cell density, (*d*) cell velocity. Parameter values and details of numerical solution are given in Höfer *et al.* (1995*b*). The numerically determined wave speed in the full model is about 4% lower than for the clamped cell density; the u and v profiles are approximately the same in both cases.

et al. (1995*a*) was formulated is amenable to many standard techniques of mathematical analysis that cannot be applied to the discrete formulation of Dallon and Othmer. This analysis was presented by Höfer *et al.* (1995*b*), and enables the separation of the cell streams during *D. discoideum* aggregation to be predicted in terms of model parameters. Most significantly, this predicts that stream separation increases with the chemotactic parameter χ, with streams not appearing if χ is less than a critical value. Höfer *et al.* (1995*b*) derived a simple formula for the dependence of this initial value on other parameters, suggesting a range of possible experimental tests.

DISCUSSION

The formation of cell streams is arguably the most visible outcome of *D. discoideum* aggregation. Both the Höfer *et al.* and Dallon–Othmer

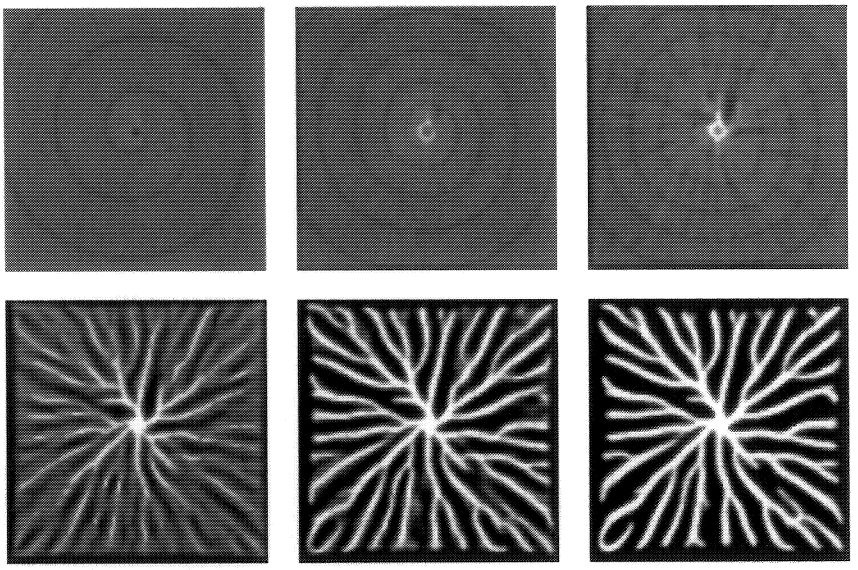

(a)

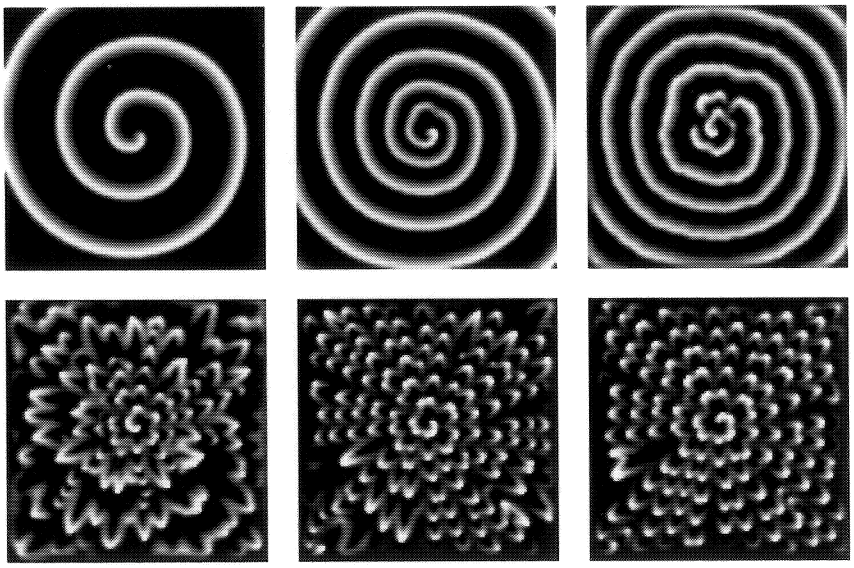

(b)

Fig. 4. Spatiotemporal evolution of (*a*) cell density and (*b*) cAMP concentration in a numerical simulation of (3,1). Solutions are plotted every 12 minutes. The initial conditions were chosen to be a plane wavefront with a free end at the centre of the domain and homogeneous cell density, with random perturbations (±7.5%) throughout. Boundary conditions are zero flux. Parameter values and details of numerical solution are given in Höfer *et al.* (1995*b*).

mathematical models predict that this behaviour is the combined results of cAMP signalling and chemotaxis. Intuitively, the streams arise because cells both produce cAMP and move up cAMP gradients; therefore, a region of high cell density will produce cAMP at high levels, thus inducing surrounding cells to move towards the region of higher density. This is an autocatalytic mechanism that leads to stream formation. The models differ in their prediction of the extent of initial aggregation required to produce this pattern. In the Höfer *et al.* model, very slight degrees of streaming are rapidly reinforced, while Dallon and Othmer predict that a more pronounced initial pattern is required. This is an experimentally testable difference, since in the latter case, a fairly uniform initial distribution of cells would aggregate without stream formation.

A number of other mathematical models have been proposed for the aggregation phase of *D. discoideum* modelling. The continuum models of Vasiev *et al.* (1994) and van Oss *et al.* (1996) are particularly relevant to our considerations, since they propose a rather different mechanism for stream formation, in which the dependence of the speed of cAMP waves on cell density is the key phenomenon. This would imply that the directed movement of cells is less significant than their effect on cAMP wave speed. Recently, Höfer and Maini (1997) have attempted to investigate this alternative via a mathematically simpler 'caricature' model, concluding that while this density-dependent speed may contribute to the streaming phenomenon, it is not consistent as an underlying explanation. A very different mathematical model has been proposed by Savill and Hogeweg (1997), focussing on the role of direct cell–cell adhesion in *D. discoideum* morphogenesis, a phenomenon neglected in the models we have discussed. They show that this provides a quite distinct potential explanation for the formation of cell streams, although precise predictions are difficult because of an absence of appropriate data on which to base parameter values. Were such data available, their model could potentially be combined with that of Dallon and Othmer (1997), since it is also based on a discrete representation of the amoebae.

Aggregation in *D. discoideum* is an elegant example of complex behaviour coordinated by microbial signalling. At the heart of the process are the 'excitability' of extracellular cAMP kinetics and the chemotactic response of *D. discoideum* amoebae to cAMP gradients. Many experimental observations are direct consequences of these two processes. An instructive example of this is the affect of reducing the extent to which cAMP activates its own secretion, which decreases the degree of cAMP excitability. Experimentally, this can be achieved by the addition of caffeine, and causes cellular aggregation to occur around a central hole, rather than as a solid mound (Siegert & Weijer, 1989). The majority of mathematical models simulate this phenomenon (Höfer *et al.*, 1995*a*; van Oss, 1996; Dallon & Othmer, 1997), confirming that it is a simple consequence of their basic common ingredients, namely excitability

and chemotaxis. Similarly, the positive correlation between wave speed and spatial wavelength, which is observed experimentally (Gross *et al.*, 1974), is a prediction shared by most models, including those of Dallon and Othmer and Höfer *et al.* In contrast, predicted explanations for cell streaming show more variation, suggesting that it represents a more delicate balance of the interaction between biochemical signalling and cell mechanics. Mathematical models provide an excellent vehicle for investigation of such interactions, with a strong track record within *D. discoideum* biology. The combination of this, and the high volume of experimental work on *D. discoideum*, suggests that the next few years will yield exciting developments in understanding *D. discoideum* morphogenesis.

ACKNOWLEDGEMENTS

JCD thanks Hans Othmer for his help and support. JAS, JCD and PKM were supported in part by grant GR/K71394 from EPSRC, and by a grant from the London Mathematical Society (scheme 3). TH acknowledges support from the Boehringer Ingelheim Fonds.

REFERENCES

Alcantara, F. & Monk, M. (1974). Signal propagation during aggregation in the slime mold *Dictyostelium discoideum*. *Journal of General Microbiology*, **85**, 321–34.

Bonner, J. T. (1982). Comparative biology of cellular slime molds. In *The Development of* Dictyostelium discoideum, ed. W. F. Loomis, pp. 1–33. Academic Press.

Collier, J. R., Monk, N. A. M., Maini, P. K. & Lewis, J. H. (1996). Pattern formation by lateral inhibition with feedback: a mathematical model of delta–notch intercellular signalling. *Journal of Theoretical Biology*, **183**, 429–46.

Dallon, J. C. & Othmer, H. G. (1997). A discrete cell model with adaptive signalling for aggregation of *Dictyostelium discoideum*. *Philosophical Transactions of the Royal Society of London, Series B*, **352**(1357), 391–417.

Devreotes, P. N. (1982). Chemotaxis. In *The Development of* Dictyostelium discoideum, ed. W. F. Loomis, pp. 117–68. Academic Press.

Goldbeter, A. & Segel, L. A. (1977). Unified mechanism for relay and oscillations of cyclic AMP in *Dictyostelium discoideum*. *Differentiation*, **17**, 127–35.

Grindrod, P. (1991). *Patterns and Waves*. Oxford University Press.

Gross, J. D., Peacey, M. J. & Trevan, D. J. (1974). Signal emission and relay propagation during early aggregation in *Dictyostelium discoideum*. *Journal of Cell Science*, **22**, 645–56.

Hagan, P. S. & Cohen, M. S. (1981). Diffusion induced morphogenesis in the development of *Dictyostelium*. *Journal of Theoretical Biology*, **93**, 881–908.

Höfer, T. & Maini, P. K. (1997). Streaming instability of slime mold amoebae: an analytical model. *Physical Review E*, **56**, 2074–80.

Höfer, T., Maini, P. K., Sherratt, J. A., Chaplain, M. A. J., Chauvet, P., Metevier, D., Montes, P. C. & Murray, J. D. (1994). A resolution of the chemotactic wave paradox. *Applied Mathematics Letters*, **7**, 1–5.

Höfer, T., Sherratt, J. A. & Maini, P. K. (1995*a*). *Dictyostelium discoideum*: cellular self-organization in an excitable biological medium. *Proceedings of the Royal Society of London, Series B*, **259**, 249–57.

Höfer, T., Sherratt, J. A. & Maini, P. K. (1995*b*). Cellular pattern formation during *Dictyostelium* aggregation. *Physica D*, **85**, 425–44.

Levine, H., Tsimring, L. & Kessler, D. (1997). Computational modeling of mound development in *Dictyostelium*. *Physica D*, **106**, 375–88.

Martiel, J. L. & Goldbeter, A. (1984). Oscillations and relay of cAMP signals in *Dictyostelium discoideum*: Analysis of a model based on the modification of the cAMP receptors. *Comptes Rendu des Seances de Academie des Sciences de Paris*, **298, Series III**, 549–52.

Meinhardt, M. (1983). A model for the prestalk/prespore patterning in the slug of the slime mold *Dictyostelium discoideum*. *Differentiation*, **24**, 191–202.

Murray, J. D. (1989). *Mathematical Biology*. Springer-Verlag.

Odell, G. M. & Bonner, J. T. (1986). How the *Dictyostelium discoideum* grex crawls. *Philosophical Transactions of the Royal Society of London, Series B*, **312**, 487–525.

Raman, R. K., Hashimoto, Y., Cohen, M. H. & Robertson, A. (1976). Differentiation for aggregation in the cellular slime molds: the emergence of autonomously signalling cells in *Dictyostelium discoideum*. *Journal of Cell Science*, **21**, 243–59.

Ross, F. M. & Newell, P. C. (1981). Streamers: chemotactic mutants of *Dictyostelium discoideum* with altered cyclic GMP metabolism. *Journal of General Microbiology*, **127**, 339–50.

Savill, N. J. & Hogeweg, P. (1997). Modelling morphogenesis: from single cells to crawling slugs. *Journal of Theoretical Biology*, **184**, 229–35.

Siegert, F. & Weijer, C. J. (1989). Digital image processing of optical density wave propagation in *Dictyostelium discoideum* and analysis of the effects of caffeine and ammonia. *Journal of Cell Science*, **93**, 325–35.

Soll, D. R., Wessels, D. & Sylwester, A. (1993). The motile behavior of amoebae in the aggregation wave in *Dictyostelium discoideum*. In *Experimental and Theoretical Advances in Biological Pattern Formation*, ed. H. G. Othmer, P. K. Maini & J. D. Murray. London: Plenum.

Tang, Y. H. & Othmer, H. G. (1994). A G-protein-based model of adaptation in *Dictyostelium discoideum*. *Mathematical Biosciences*, **120**, 25–76.

Tang, Y. H. & Othmer, H. G. (1995). Excitation, oscillations and wave propagation in a G-protein based model of signal transduction in *Dictyostelium discoideum*. *Philosophical Transactions of the Royal Society of London, Series B*, **349**, 179–95.

Tomchick, K. & Devreotes, P. N. (1981). Adenosine 3′,5′-monophosphate waves in *Dictyostelium discoideum*: a demonstration by isotope dilution fluorography. *Science*, **212**, 443–6.

Tyson, J. J., Alexander, K. A., Manoranjan, V. S. & Murray, J. D. (1989). Spiral waves of cyclic AMP in a model of slime mold aggregation. *Physica D*, **32**, 327–61.

van Oss, C., Panfilov, A. V., Hogeweg, P., Siegert, F. & Weijer, C. J. (1996). Spatial pattern formation during aggregation of the slime mould *Dictyostelium discoideum*. *Journal of Theoretical Biology*, **181**, 203–13.

Varnum, B., Edwards, K. B. & Soll, D. R. (1985). *Dictyostelium* amoebae alter motility differently in response to increasing versus decreasing temporal gradients of cAMP. *Journal of Cell Biology*, **101**, 1–5.

Vasiev, B., Siegert, F. & Weijer, C. J. (1997). A hydrodynamic model for *Dictyostelium discoideum* mound formation. *Journal of Theoretical Biology*, **184**, 441.

Vasiev, B. N., Hogeweg, P. & Panfilov, A. V. (1994). Simulation of *Dictyostelium discoideum* aggregation via reaction-diffusion model. *Physical Review Letters*, **73(23)** (December), 3173–6.

Weliky, M., Minsuk, S., Keller, R. & Oster, G. (1991). Notochord development in *Xenopus laevis*: simulation of cell behaviour underlying tissue convergence and extension. *Development*, **113**, 1231–44.